



HAL
open science

Automated classification of early afterdepolarizations grades in flipr calcium assays

Levy Batista, Ricardo Contu, Brittney van Hese, Fabian Zanella, Thierry Bastogne

► **To cite this version:**

Levy Batista, Ricardo Contu, Brittney van Hese, Fabian Zanella, Thierry Bastogne. Automated classification of early afterdepolarizations grades in flipr calcium assays. Annual Meeting of Safety Pharmacology Society, SPS 2018, Sep 2018, Washington DC, United States. hal-01925678

HAL Id: hal-01925678

<https://hal.science/hal-01925678v1>

Submitted on 17 Nov 2018

HAL is a multi-disciplinary open access archive for the deposit and dissemination of scientific research documents, whether they are published or not. The documents may come from teaching and research institutions in France or abroad, or from public or private research centers.

L'archive ouverte pluridisciplinaire **HAL**, est destinée au dépôt et à la diffusion de documents scientifiques de niveau recherche, publiés ou non, émanant des établissements d'enseignement et de recherche français ou étrangers, des laboratoires publics ou privés.

AUTOMATED CLASSIFICATION OF EARLY AFTERDEPOLARIZATIONS GRADES IN FLIPR CALCIUM ASSAYS

L. BATISTA¹, R. CONTU², B. VAN HESE², F. ZANELLA², T. BASTOGNE^{1,3,4}
¹CYBERnano, ²STEMONIX, ³CRAN UL-CNRS UMR 7039, ⁴INRIA BIGS

Objectives

The detection and classification of proarrhythmic phenotypes like **early afterdepolarizations (EADs)** is fundamental in the safety pharmacology assessment of developing drugs. Calcium flux analysis enables sensitive and high throughput in vitro assays to assess potential cardiac liabilities of compounds of interest in cardiomyocytes, generating large amounts of multi-parametric data in a single experiment. However, instrument-agnostic, robust automated data analysis platforms to **predict and characterize EADs** are not readily available.

Methods

We developed a **new integrated approach able to automatically classify severity grades of EADs observed in high throughput calcium flux data**. **Stemonix microHeart** screening plates promote cardiomyocyte alignment and enable greater resolution over the analysis of pro-arrhythmic phenotypes observed in human induced pluripotent stem cell-derived cardiomyocytes (hiPSC-CMs). hiPSC-CMs were maintained in standard or microengineered microHeart 384-well screening plates for seven days prior to compound treatment and calcium flux analysis. Compound responses were categorized into 7 phenotypes: normal rhythmic calcium flux behavior, **five severity grades of EADs**, and cessation of beating activity (quiescence). Data generated in the microHeart platform was used by Cybernano to develop and validate a statistical learning algorithm: **Cybernano i-Cardio EAD** to characterize transient patterns associated with different classes of EADs. Parametric modeling of the beating pattern was associated with a numeric degree of EADs with a value normalized between 0 (no beating) and 1 (no EAD). Finally, a multiclass classification is applied to discriminate the five severity grades of EADs.

Results

EAD classifications obtained from standard manual data plotting were compared to classifications obtained with Cybernano algorithms, and concordance between the datasets was analyzed for validation. Robust concordance was observed through this analysis, indicating that the algorithm has satisfactory fidelity to streamline data analysis for automated detection of EADs from high throughput calcium flux analysis in cardiomyocytes.

Conclusion

In summary, the comparison of data analysis obtained have demonstrated the **proof of concept and very promising perspectives for automatic detection and grading EADs** in high throughput calcium flux assays. This comparative study will serve as basis for extending the analysis to a larger library of molecules for additional validation.

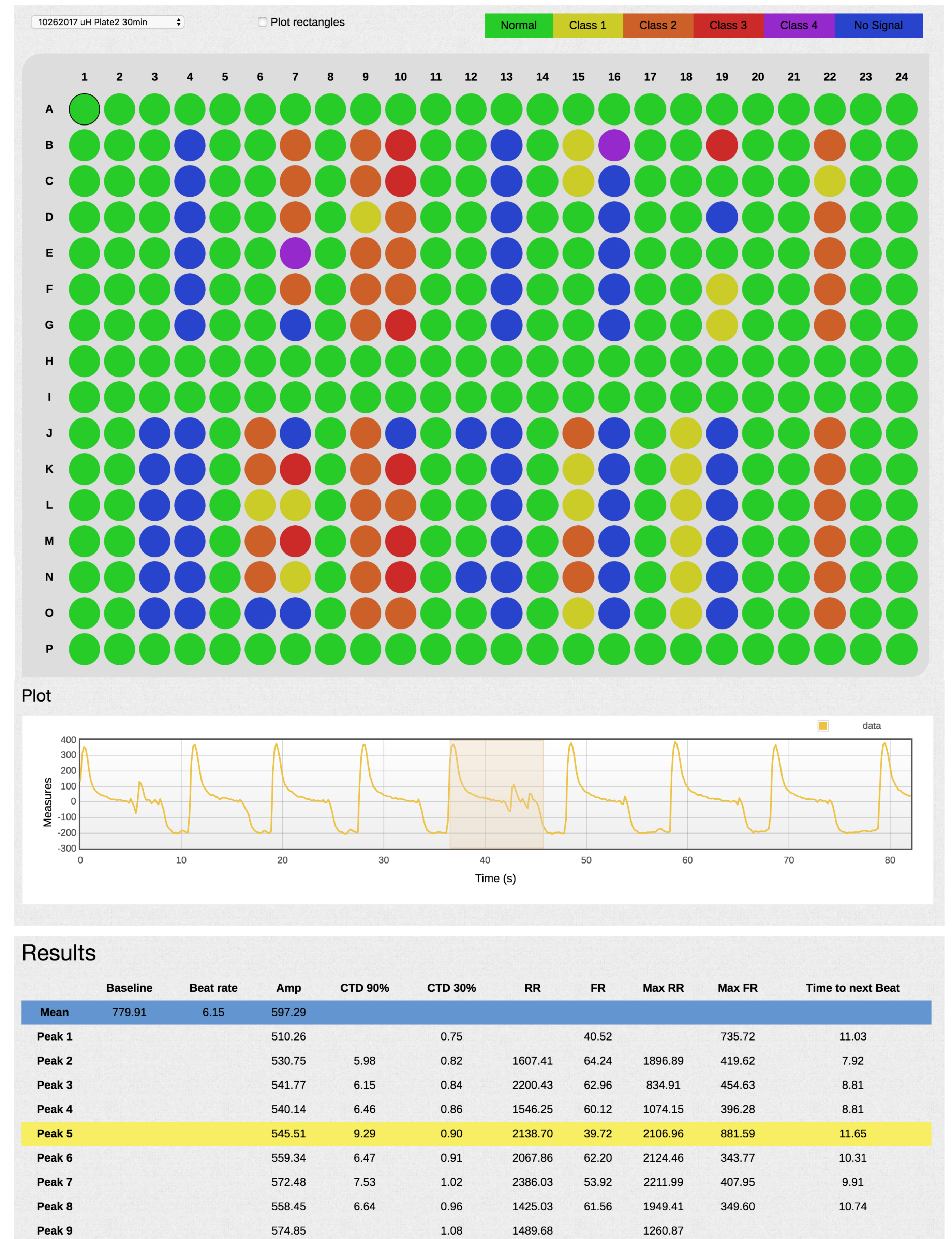


Fig.1: Example of i-Cardio EAD report obtained from FLIPR data of a 384-well screening plate. Each colour corresponds to a EAD severity grade on a scale composed of 5 levels.

		PREDICTED						
		Normal	EAD-1	EAD-2	EAD-3	EAD-4	No Signal	Undefined
TRUE	Normal	1265	3	0	0	0	3	0
	EAD-1	1	34	6	1	0	0	0
	EAD-2	0	7	49	2	0	0	0
	EAD-3	0	0	13	18	0	1	4
	EAD-4	0	0	0	4	4	1	0
	No Signal	0	0	0	0	0	81	0
Undefined	0	0	0	6	0	17	16	

Fig.2: Confusion matrix presenting the performances of the automatic EAD classification

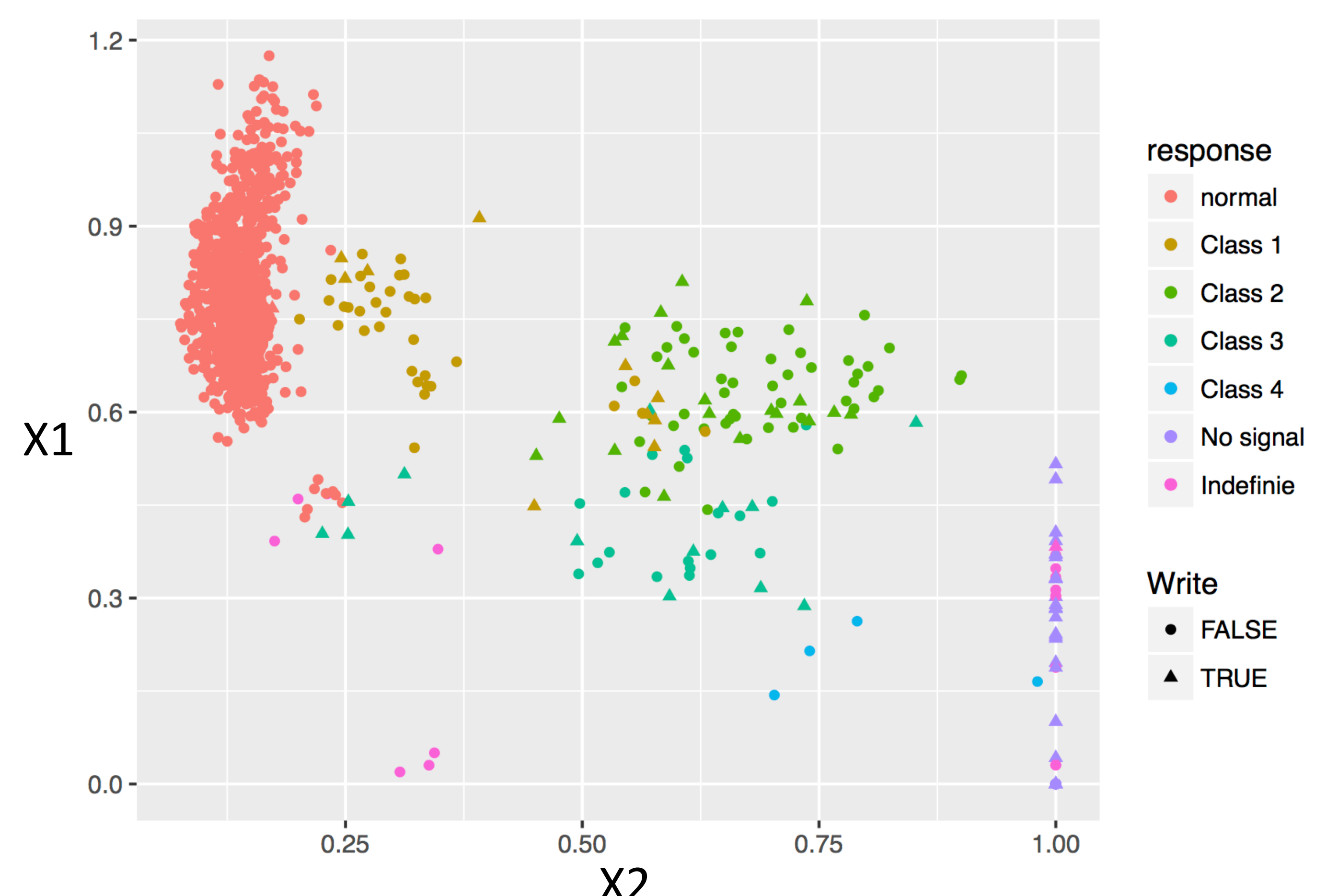


Fig.3: Visualization of the EAD classes in a 2D-space associated with 2 classifiers: X1 and X2.